

# CHALMERS



## Further development, implementation and testing of scanning mini-DOAS instruments for use on high latitude volcanoes and volcanic gas emission monitoring at volcano Telica, Nicaragua

*Master's Thesis within the Radio and Space Sciences Master's Programme*

Daniel Nilsson

Supervisor: *Bo Galle*

Department of Earth and Space Sciences  
CHALMERS UNIVERSITY OF TECHNOLOGY  
Gothenburg, Sweden, 5th of July 2013

**Further development, implementation and testing of scanning mini-DOAS instruments for use on high latitude volcanoes and volcanic gas emission monitoring at volcano Telica, Nicaragua**  
DANIEL NILSSON

©DANIEL NILSSON

Master's Thesis within the Radio and Space Sciences Master's Programme

Department of Earth and Space Sciences  
Chalmers University of Technology  
412 96 Gothenburg

## Abstract

Reliable volcanic gas emission monitoring is crucial when trying to create an understanding of the geophysical processes of volcanoes, and may as well prove a key ingredient in risk assessment. One of the prominent instruments used for volcanic gas flux measurements today is the mini-DOAS instrument, a ground-based optical remote sensing instrument utilizing a UV-spectrometer.

Within this thesis, modifications of the mini-DOAS instrument are tested and implemented in order to increase performance at high latitude volcanoes. As the solar elevation angle is lower at high latitudes, less solar UV-light is available because of atmospheric absorption. Replacement of the Ocean Optics S2000 spectrometer with the Ocean Optics Maya2000 Pro is tested, as the Maya2000 has a higher sensitivity to UV-light. Promising results shows that a change of spectrometer at measurement stations by high latitude volcanoes will allow for measurements during a longer time of the day, as well as significantly reduced error levels in the measurements.

To get experience working with the mini-DOAS instruments, a field campaign was carried out at the volcano Telica (Nicaragua). The campaign exploited a set of rapid deployment scanning mini-DOAS instruments as well as a mobile DOAS system used for traverses in order to gather data on the SO<sub>2</sub> flux of the volcano. Calculated flux indicated an increase in the activity of the volcano. Results from this campaign was later used in a larger study of multidisciplinary observations during the 2011 explosive eruption of the volcano.

**Keywords:** DOAS, sulfur dioxide, volcano monitoring, high latitude volcanoes, UV-spectroscopy

# Contents

<b>1</b>	<b>Introduction</b>	<b>1</b>
1.1	Why measure gas emissions from volcanoes? . . . . .	1
1.2	DORSIVA, NOVAC and FutureVolc projects . . . . .	1
1.3	Aims and goals of this project . . . . .	2
1.4	Field campaign: Telica . . . . .	3
1.4.1	Previous field campaign . . . . .	3
<b>2</b>	<b>Measuring volcanic gas emissions</b>	<b>5</b>
2.1	Differential Optical Absorption Spectroscopy . . . . .	5
2.2	DOAS evaluation in practice . . . . .	7
2.2.1	The spectrometer . . . . .	7
2.2.2	Evaluation routine . . . . .	8
2.2.3	Calibration and reference spectra . . . . .	10
2.2.4	Filtering . . . . .	10
2.3	What gases to measure? . . . . .	10
2.3.1	Ozone . . . . .	11
2.3.2	Ring effect . . . . .	11
2.3.3	Spectroscopic properties of SO <sub>2</sub> . . . . .	11
2.4	Volcanic gas flux measurement strategies . . . . .	12
2.4.1	Making traverses using a mobile spectrometer . . . . .	12
2.4.2	Scanning the plume using a stationary spectrometer . . . . .	13
<b>3</b>	<b>Mini-DOAS instruments and software</b>	<b>16</b>
3.1	Software: MobileDOAS and NOVAC Program . . . . .	16
3.2	Mobile DOAS . . . . .	16
3.3	Scanning mini-DOAS . . . . .	17
3.4	Modifications of the scanning mini-DOAS instrument to better suit high latitude volcanoes . . . . .	18
3.4.1	Replace rotating hood with a quartz cylinder . . . . .	19
3.4.2	Replacing the S2000 with the Maya2000 Pro spectrometer . . . . .	21
<b>4</b>	<b>Test results for the Maya2000 Pro</b>	<b>23</b>
4.1	Results: exposure time and column error . . . . .	23
4.2	Results: wavelength misalignment . . . . .	25
<b>5</b>	<b>Field campaign at Telica, Nicaragua</b>	<b>27</b>
5.1	Scanning mini-DOAS measurements . . . . .	27
5.2	Mobile mini-DOAS measurements . . . . .	29
5.3	Wind speed data . . . . .	29
<b>6</b>	<b>Results from the field campaign at Telica</b>	<b>31</b>
<b>7</b>	<b>Conclusions and discussion</b>	<b>34</b>
7.1	Instrument modifications . . . . .	34
7.2	Field campaign at Telica . . . . .	35
	<b>References</b>	<b>36</b>

# 1 Introduction

Throughout the world there are more than 500 active volcanoes, ranging up to 1,500 depending on the definition of active. A majority of those volcanoes are situated within the “Ring of Fire”, an area surrounding the Pacific Ocean reaching from the southern part of Chile all along the American West Coast, Alaska, Kamchatka, throughout South East Asia and all the way to New Zealand.

Monitoring of active volcanoes has been of high interest for a long time and many of the common monitoring methods dates back to methods developed by the Hawaiian Volcano Observatory (HVO), established in 1912. When it comes to optical remote sensing methods for gas emission measurements, it all started out on a larger scale with the introduction of the mask correlation spectrometer, COSPEC, in the 1960s (Hoff & Millán, 1981). Later on DOAS (differential optical absorption spectroscopy) techniques were developed (Platt & Stutz, 2008), with the first DOAS volcanic gas emission measurements taking place in 1992 (Edner, 1994). Details regarding the principles behind those methods will be presented later (see chapter 2).

In 2001, the mini-DOAS instrument was introduced as a small and highly affordable complement to COSPEC (Galle, 2003) and since then it has successfully been used to monitor volcanic, as well as anthropogenic, gas emissions. (Johansson *et al.*, 2008), (Johansson, 2009), (Rivera, 2009)

## 1.1 Why measure gas emissions from volcanoes?

It is important to measure gas emissions from volcanoes for a number of reasons. One of the most fundamental reasons is to simply get a better understanding of the geophysical processes in volcanoes. As the temperature and pressure changes in the magma below the volcano, the solubility of gases in the magma changes and degassing will occur. By measuring the gases emitted from volcanoes, volcanologists are presented with an additional tool in the work to try to understand important mechanisms surrounding volcanoes. As a consequence of better understanding of volcanic behavioural patterns, risk assessment can be improved, potentially saving both lives and resources.

Another important reason to measure volcanic gas emissions is that heavy emissions may have a strong environmental impact, not only on a local scale but also in a regional or global perspective (Stoiber *et al.*, 1987). Some effects caused by volcanoes reaches from volcanic gases being directly harmful and toxic on a local scale while emissions may cause a significant impact on the global climate.

As it may not be possible to perform *in situ* gas emission measurements on all active volcanoes worldwide collected data from a small number of volcanoes can be used for validation of satellite based gas emission measurements. By validating satellite measurements, much better estimates of the total global volcanic gas emissions can be done.

## 1.2 DORSIVA, NOVAC and FutureVolc projects

The scanning (dual-beam) mini-DOAS instrument (Johansson *et al.*, 2009) was introduced as a small and highly affordable complement to COSPEC within the EU-project DORSIVA (Galle *et al.*, 2006). It has since then successfully been

used to monitor volcanic – as well as anthropogenic – gas emissions, providing yet another important parameter for the observatories to perform e.g. risk assessment and gas emission estimates.

Within the EU-project NOVAC, mini-DOAS instruments and related equipment have been deployed on a number of volcanoes worldwide to form a global volcano monitoring network (Galle *et al.*, 2011). The goal of the NOVAC project was to establish a global network with the purpose to perform quantitative volcanic gas emission measurements. This is done by utilizing the unique features of the scanning mini-DOAS instrument, namely the ability to perform real-time automatic, unattended volcanic gas emission measurements with high time resolution (Galle, 2010).

As the next step in global volcanic monitoring, a rapid deployment scanning mini-DOAS instrument was developed for use in emergencies and other situations where measurements have to be performed with short notice (Conde, 2013). The rapid deployment NOVAC systems utilizes a satellite link for communication and can be deployed with full coverage within a day, given good installation sites are available and accessible.

At the end of 2012, the 3.5 year long FutureVolc project was formally initiated. The project is described on the FutureVolc website (Futurevolc, 2013):

The main objectives of FutureVolc are to establish an integrated volcanological monitoring system through European collaboration, develop new methods to evaluate volcanic crises, increase scientific understanding of magmatic processes and improve delivery of relevant information to civil protection and authorities.

Part of this thesis is included in the FutureVolc project, as a high latitude version of the scanning mini-DOAS instrument is developed, deployed and tested with the intent to be better suited for the conditions on Icelandic (and other high latitude) volcanoes.

### 1.3 Aims and goals of this project

A vast majority of the volcanoes monitored within the NOVAC project are located in or in the vicinity of the equatorial region. This may be somewhat optimal from a measurement point of view, as the amount of scattered UV light is higher in this region due to the higher solar elevation angle. However, it also reflects upon the fact that the current instruments are not as suitable for high latitude volcanoes. The two most substantial factors as to why the current instrument implementation is suboptimal at high latitude volcanoes are the lower temperatures during winter and – possibly more important – the low amount of scattered UV light available in high latitudes.

As the scanning mini-DOAS instruments are starting to get installed at high latitude volcanoes on Iceland or in Kamchatka the need for a better suited instrument have grown stronger. The aim of this thesis is to modify the current scanning mini-DOAS instruments in order to develop, implement and test a system better suited for at high latitude volcanoes. The main focus will be to examine the possibilities to replace the current spectrometer with a spectrometer that is more sensitive to UV light. Mechanical disadvantages of the current scanner will also be addressed in order to develop a scanner better suited for the harsh winter conditions.

Originally, the goal was to eventually install and test the modified scanning mini-DOAS system in a real-life situation at a volcano on Iceland. One of the motivations behind such a field campaign, apart from actually getting to test the new systems, was to get experience from actually working with the instruments in the field. One disadvantage of doing a field campaign on Iceland is that volcanoes on Iceland typically does not have any noticeable gas emissions when there is no eruptive activity. During spring 2011, an opportunity to carry out a field campaign at the volcano Telica in Nicaragua appeared. Indications of increased activity at Telica, in combination with a good opportunity to obtain field experience, led to the decision to carry out the field campaign at Telica and to suspend the campaign to Iceland indefinitely. The field campaign to Telica was funded by a Minor Field Study (MFS) grant from Sida (Swedish International Development Cooperation Agency).

While the purpose of the field campaign at Telica was to obtain needed field experience on a personal level, it also presented a good opportunity to do follow-up work on a previous field campaign at Telica. It also served to provide INETER with important information about Telica.

## **1.4 Field campaign: Telica**

Towards the end of May 2011 INETER (Instituto Nicaragüense de Estudios Territoriales) reported that there were indications of an increase in the activity of the volcano Telica in Nicaragua. The volcano is located approximately 20 km north of León, which is the second largest city in Nicaragua. After contact between INETER and researchers at Chalmers University of Technology a field campaign at Telica was initiated. The first stage of this field campaign was to install two spectrometers from the rapid deployment system developed within the NOVAC project and the second stage was to conduct additional measurements by doing traverses using a mobile spectrometer.

As the volcano previously had been the subject of field work during the development of the rapid deployment system, a lot of the prerequisites were already sorted out including suitable locations to install spectrometers and scanners with regard to e.g. wind direction.

### **1.4.1 Previous field campaign**

Between December 2009 and March 2010 the first continuous gas flux measurement at Telica took place as a part of a campaign to test the, by then, recently developed rapid deployment system. During this campaign three locations suitable for scanning DOAS measurements were chosen, with respect taken to accessibility, security and plume visibility.

The predominant wind direction during this campaign was found to be 90° and the plume height varied between 500 m and 2000 m (above sea level). The three measurement stations were positioned at an altitude of 215 m, 232 m and 257 m and the crater has an altitude of 1061 m.

In the results from this campaign, a shorter period of eleven days in the middle of January 2010 were identified where the average flux showed a significant increase. Before January 11 the average daily flux was 75 t/d, while the average daily flux between January 11 and January 21 was as high as 328 t/d

with most days having an average above 200 t/d. After January 21 the average daily flux went down to 104 t/d.

## 2 Measuring volcanic gas emissions

When trying to gather data on volcanic gas emissions there is a number of different methods available. Typically, those are divided into three categories: measuring dissolved volatiles in rocks and inclusions surrounding the volcano, direct sampling of the gas and remote sensing techniques. Which one is the most suitable heavily depends on the purpose of the measurement and the accessibility of the areas surrounding the volcano.

When the goal is to determine the composition of volcanic emissions it is preferable to work with a direct sample or rock and inclusion samples. This holds true especially when trying to detect trace gases as the sample can be examined in a clean laboratory environment. When it comes to quantitative measurements, such as measuring  $\text{SO}_2$  flux, it is suitable to work with some of the different remote sensing techniques available. Here we find a range of different spectroscopic methods, such as FTIR (Fourier transform infrared spectroscopy) and DOAS.

This chapter gives a general explanation of the DOAS technique in section 2.1 followed by a more specific explanation of how the DOAS technique is applied in section 2.2. A brief explanation to the choice of gases to measure is found in section 2.3. After this, two typical DOAS measurement strategies are described in section 2.4. The current implementation of these techniques and strategies for use in volcanic gas emission monitoring is described in chapter 3, along with suggested modifications to improve measurements at high latitude volcanoes.

### 2.1 Differential Optical Absorption Spectroscopy

The basic principle behind DOAS is the Beer-Lambert law, which states that the intensity,  $I(\lambda)$ , of light decreases exponentially with the distance as it passes through an absorbing medium. The decrease depends on the number density,  $N$ , of the absorbing substance as well as its absorption cross section,  $\sigma(\lambda)$ , where  $\lambda$  is the wavelength. That is:

$$I(\lambda) = I_0(\lambda) \cdot \exp[-L\sigma(\lambda)N], \quad (1)$$

where  $L$  is the distance traveled through the medium and  $I_0$  is the initial intensity before it enters the medium.

If there's more than one absorbing component in a medium, each with a different cross section, the above expression becomes:

$$I(\lambda) = I_0(\lambda) \cdot \exp\left[-L \sum_i \sigma_i(\lambda)N_i\right]. \quad (2)$$

The (negative) exponent is usually called the optical density, denoted  $\tau(\lambda)$ , and can be expressed as:

$$\tau(\lambda) \equiv \ln \frac{I_0(\lambda)}{I(\lambda)} = L\sigma(\lambda)N \quad (3)$$

Theoretically, one can determine the composition of a sample by measuring the absorption of the sample using light from some source (typically the incident sunlight), given the cross sections of all the species found in the sample are

known. In practice, however, this is not as feasible as it might sound, as there are many other elements affecting the results of the measurements. Instruments and equipment used in the measurements, e.g. spectrometers and lenses, may influence the measurement and is often introduced as an instrument factor,  $A(\lambda)$ .

Additionally, when performing atmospheric measurements there are other sources of extinction in the atmosphere that influence the amount of light transmitted, such as scattering. Typically one has to consider Rayleigh scattering and Mie scattering, and those can be accounted for in the Beer-Lambert law by introducing the corresponding extinction factors,  $\varepsilon_R(\lambda)$  and  $\varepsilon_M(\lambda)$ . Thus, the expression for the transmitted light becomes:

$$I(\lambda) = I_0(\lambda) \cdot \exp \left[ -L \left( \varepsilon_R(\lambda) + \varepsilon_M(\lambda) + \sum_i \sigma_i(\lambda) N_i \right) \right] \cdot A(\lambda) \quad (4)$$

In most real cases several of the above factors can be considered unknown and solving for e.g. number density (or, in a laboratory setting, for the cross section) can prove close to impossible. At this point, the beauty of the DOAS technique becomes apparent. The DOAS technique uses the fact that most of the above factors are to be considered broad-band (i.e. slow variations with respect to wavelength) while many of the atmospheric trace gases have narrow-band absorption structures. The molecular absorption cross section can be divided in two parts:

$$\sigma_i(\lambda) = \sigma'_i(\lambda) + \sigma_{iS}(\lambda), \quad (5)$$

where  $\sigma_{iS}(\lambda)$  is the broad-band variations and  $\sigma'_i(\lambda)$  is the narrow-band parts, also known as the *differential cross section*. If we then insert (5) into (4) we get:

$$I(\lambda) = I_{0S}(\lambda) \cdot \exp \left( -L \sum_i \sigma'_i(\lambda) N_i \right), \quad (6)$$

where  $I_{0S}(\lambda)$  represents the broad-band features, namely:

$$I_{0S} = I_0(\lambda) \cdot \exp \left[ -L \left( \varepsilon_R(\lambda) + \varepsilon_M(\lambda) + \sum_i \sigma_{iS}(\lambda) N_i \right) \right] \cdot A(\lambda) \quad (7)$$

Here, the true power of the DOAS technique comes into play. If the only difference between two spectra were the presence of a species, equation (3) could have been used straight away to get the relative column density of that species. As it is almost never the case that the only thing that has changed between the acquisition of two spectra is the amount of a single species, this does not work. Instead we use the above expression with our previous definition of optical density and define a differential optical density:

$$\tau'(\lambda) \equiv \ln \left( \frac{I_{0S}(\lambda)}{I(\lambda)} \right) = L \sum_i \sigma'_i(\lambda) N_i \quad (8)$$

Here,  $LN_i$  represents the column density of each absorbing component. So, in order to obtain the relative column density between two spectra we need

to first find the differential optical density for each spectra. It can then be determined by minimizing the difference between measured differential optical density and the differential optical density obtained using differential optical cross sections from literature. That is:

$$\min \left\| \tau'(\lambda) - L \sum_i \sigma'_i(\lambda) N_i \right\|, \quad (9)$$

and as almost all unwanted changes between to aquired spectra only contributes with broad-band features, they can easily be removed.

The removal of broad-band features varies between different implementations of the DOAS technique. Common methods to do this is either by mathematical high pass filtering or by fitting a polynomial to the slowly varying portion of the spectra and subtract it.

It should be noted that not only broad-band features in the unwanted elements are removed, but it comes with the cost that broad-band features in the cross section of the species that should be measured also are removed.

## 2.2 DOAS evaluation in practice

When implementing the DOAS measurement technique a number of considerations has to be taken into account. Here follows a brief overview of the DOAS evaluation process – as it is done within the NOVAC project – to give a small insight to the different steps, ranging from collecting the spectra to performing the fit.

### 2.2.1 The spectrometer

For both mobile and scanning DOAS systems, the incoming spectra is collected using a spectrometer. Today the spectrometer used in the NOVAC stations is the Ocean Optics S2000 spectrometer (or the double SD2000 spectrometer). New spectrometers are sometimes considered for testing as they enter the market, like the Ocean Optics spectrometer Maya2000 Pro that is evaluated here in order to see if it can improve measurements at high latitude volcanoes.

Below follows a list of important concepts related to the spectrometer and the actual aquisition of the spectrum as there are a number of things that needs to be considered before the DOAS evaluation process can be carried out.

**Dark current** Even when the charge-coupled device (CCD) in the spectrometer is not illuminated a small current, ingeniously enough called the *dark current*, is generated. The behaviour of this dark current can be described as exponentially decreasing with lower temperature and linearly increasing with higher exposure time. As the power budget for most of the NOVAC stations is limited, temperature control of the spectrometer is not possible. This means that the dark current can not be neglected and all spectra has to be corrected in the processing stage. This is typically done by collecting a single spectrum without having any light enter the spectrometer and then let the collected spectrum represent the dark current. It is then assumed that the dark current will be the same for all other spectra collected within a limited time span and this way it can easily be subtracted from every spectra before further processing.

**Offset and readout noise** In addition to the dark current, a number of other factors affect the measured spectra. Typically, one has to consider noise related to the readout of the signal as well as an electronic offset level in the spectrum. While it often may be possible to model readout noise and offset by making a set of elaborate measurements, the approach used here is instead to consider them a part of the dark current spectra. This way, offset (and to some extent readout noise) is automatically corrected during the dark spectrum removal stage described above. One drawback of this approach is that it requires collection of a new dark spectrum at regular intervals, as especially the offset strongly depends on temperature.

**Straylight** Sometimes light that enters the spectrometer does not hit the pixel that correspond to the wavelength of the light, which gives errors in obtained spectra. This light is generally referred to as straylight and have a number of causes. Sometimes the spectrometer allows light to enter at angles or places not intended in the design and sometimes light that originates from the intended source takes an unintended path within the spectrometer (e.g. in the presence of dust particles). Within the telescope used in the NOVAC stations there is a filter that limits the wavelengths allowed to pass through the telescope to those of the region in which the DOAS fit is performed. This is done in order to minimize the amount of unnecessary light that enters the spectrometer, reducing the amount of straylight.

**Shift and squeeze** Another unwanted behaviour found in the spectrometer is that small changes in wavelength alignment may occur, which will put the aquired spectra and the reference spectra in different wavelength-pixel-mappings. This can either be manifested by a stretch (or a squeeze) in the wavelength-pixel-mapping, or by a shift. In the NOVAC case, this is accounted for by introducing two additional parameters into the DOAS fit procedure, namely a shift and a linear squeeze. We can now re-write equation (9) as:

$$\min \left\| \tau'(\lambda) - L \sum_i \sigma'_i(\lambda + a + b(\lambda - \lambda_0))N_i \right\|, \quad (10)$$

and calculate  $a$  and  $b$  during the fit procedure. This is done by finding a set of  $a$  and  $b$  that minimizes the residual of the spectra after the fit.

### 2.2.2 Evaluation routine

The default DOAS evaluation routine implemented within the NOVAC project is the following:

1. Subtract the collected dark spectrum from all collected spectra, including the sky spectrum.
2. Remove any residual offset (typically from straylight) in all spectra by subtracting the mean value of the first channels. This is possible since these channels are not illuminated, as there is no sky light in this wavelength region.

3. Divide acquired spectra with the sky spectrum (see below) to get relative absorption spectra.
4. Remove broad-band features and obtain differential absorption by applying a high pass binomial filter (see section 2.2.4).
5. Take the logarithm of acquired spectra.
6. Calculate and/or apply shift and squeeze, if any.
7. Perform the fit of reference spectra to acquired spectra to obtain column density of measured species as described in section 2.1.

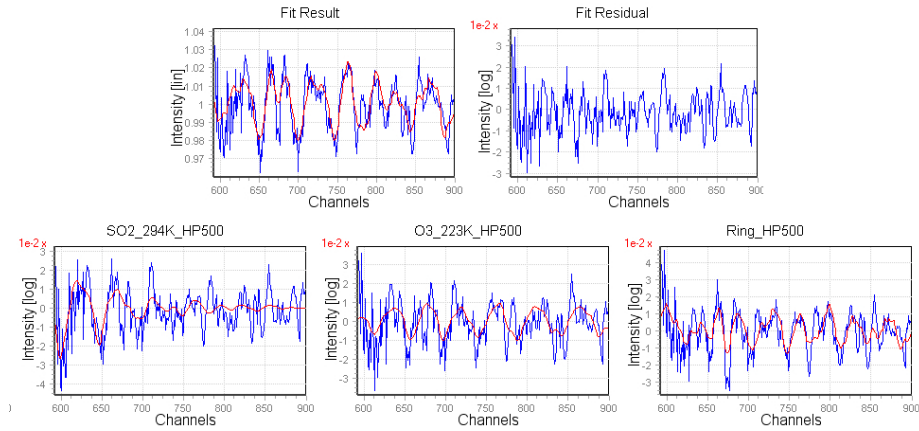


Figure 1: Showing an example of DOAS fit results. The top row shows the full fit and residual while the bottom row shows the fit of each reference species (here:  $\text{SO}_2$ ,  $\text{O}_3$  and a Ring reference).

Figure 1 shows an example of how a typical fit using  $\text{SO}_2$ ,  $\text{O}_3$  and Ring (see section 2.3.2) references would look like. The resulting fit can be seen in the top of the figure, along with the residual after the fitting of the three references has been carried out. The lower three spectra in the figure first shows the fit of  $\text{SO}_2$  along with the original DOAS processed spectrum, then the fit of  $\text{O}_3$  along with the residual after removing the  $\text{SO}_2$  features and last the fit of the ring spectrum along with the residual after  $\text{SO}_2$  and  $\text{O}_3$  have been removed.

The sky spectrum (sometimes referred to as the *Fraunhofer reference spectrum*) is a spectrum collected as a reference used by all other collected spectra during a session. This reference is used to get a relative column for the measurement and is ideally captured outside the plume and would thus correspond to a level of no volcanic gas. If the sky spectrum is collected within the plume, the offset from the true zero volcanic gas level is calculated from all collected spectra so that a proper zero gas level is obtained.

It should be noted that the software used for the evaluation does allow for some additional options as to how the evaluation should be done. For a short overview of the softwares used, see section 3.1.

### 2.2.3 Calibration and reference spectra

The spectra collected from two different spectrometers are never identical, even if the spectrometers are of the same brand, model and make. It is thus important to take into account how collected spectra will look for each particular spectrometer. The two main goals of the calibration routine used is to determine the wavelength-to-pixel mapping and to obtain the slit function of the spectrometer. This information is then used in combination with a high resolution cross section of the species to be measured in order to obtain a reference for the fitting process.

The wavelength-to-pixel mapping is determined by measuring a mercury emission spectrum and select a number of prominent peaks, for which the exact wavelength is known, in proximity of the gas fit region and then fit a third degree polynomial to the wavelength and pixel/channel values.

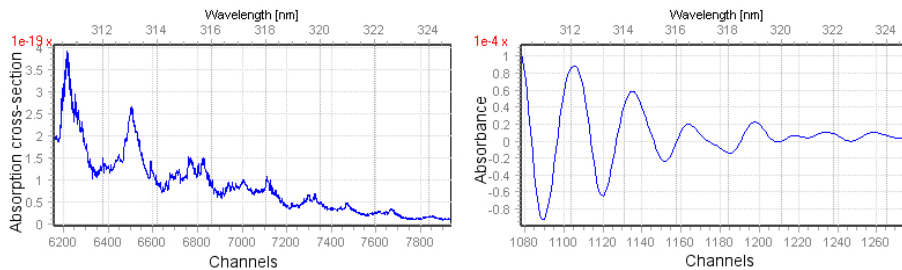


Figure 2: The raw  $\text{SO}_2$  reference spectrum to the left and to the right an example of a DOAS reference spectrum after the calibration procedure.

To obtain the slit function of the spectrometer (i.e. the way the spectrometer is broadening and measuring a single line), a peak of a single wavelength is observed. From looking at the measured spectrum, the blurring of the emission line gives the line shape function. The high resolution cross section is then convolved with the line shape function. After this the resulting spectrum is scaled to represent 1 ppm, taken as negative and exponentiated to represent an absorption spectrum according to the Beer-Lambert law (see equation (1)). To get a DOAS reference spectrum, the obtained theoretical absorption spectrum is then high pass filtered and logarithmised. An example of what the  $\text{SO}_2$  reference spectrum looks like before and after the calibration routine can be seen in figure 2.

### 2.2.4 Filtering

As briefly discussed in section 2.1, high pass filtering is used to remove broadband features in the measured spectra. In both the MobileDOAS and the NOVAC Program software, filtering is done by applying a high pass binomial. This is basically just applying a low pass binomial to the spectrum and then divide the original spectrum with the low pass filtered spectrum.

## 2.3 What gases to measure?

With the currently available set of techniques, one common approach to volcanic gas emission measurements is to monitor the flux of  $\text{SO}_2$ . This is because  $\text{SO}_2$

is usually abundant and is thus one of the easier volcanic gases to detect and measure with remote sensing techniques. The SO<sub>2</sub> flux measurements are then combined with complementary ratio measurements of other less abundant gases (e.g. HF/SO<sub>2</sub>, CO<sub>2</sub>/SO<sub>2</sub> and HCl/SO<sub>2</sub> ratios) in order to obtain their respective fluxes. Complementary techniques are typically *in situ* measurements using either FTIR or direct sampling.

### 2.3.1 Ozone

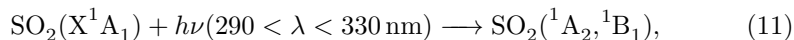
Measurements of SO<sub>2</sub> using DOAS remote sensing techniques are done in the ultraviolet region because of the spectroscopic properties of SO<sub>2</sub> (see section 2.3.3). One of the major UV region absorbers in the atmosphere is ozone (O<sub>3</sub>). Because of this, atmospheric ozone needs to be introduced in the DOAS fit procedure in order to get good results.

### 2.3.2 Ring effect

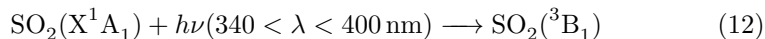
Inelastic rotational Raman scattering may cause problems when doing spectroscopic measurements of the atmosphere, especially when doing DOAS measurements on scattered light (see section 2.1). The inelastic rotational Raman scattering changes the energy of photons, resulting in a slight change of wavelength. As the number of photons in high absorption lines are much lower than outside the line, more photons are thus shifted into the line compared to the number of photons shifted out of the line. The result is a “filling in” of the absorption line (Grainger & Ring, 1962). In DOAS applications this has to be corrected for, typically by introducing a Ring reference spectrum in the DOAS fit procedure.

### 2.3.3 Spectroscopic properties of SO<sub>2</sub>

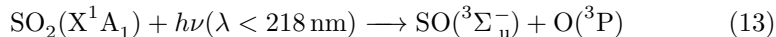
The absorption cross section of SO<sub>2</sub> is basically divided into two areas: one strong absorption section reaching from approximately 240 nm to somewhere above 330 nm and one weaker absorption section between 340 nm and 400 nm (Finlayson-Pitts & Pitts, 2000). The first and strongest absorption band originates from the following transition to singlet excited states:



while the second and weaker band comes from a spin-forbidden transition to a triplet state:



Dissociation may only occur at wavelengths shorter than 218 nm with:



with the result that there is no dissociation in the atmosphere, as wavelengths below 290 nm are not present. Using this information along with spectroscopic properties of other volcanic and atmospheric gases, a region between 310 nm and 325 nm has been chosen for the DOAS fitting of SO<sub>2</sub>.

## 2.4 Volcanic gas flux measurement strategies

Flux of volcanic gases – such as  $\text{SO}_2$ , usually expressed in kg/s or ton/day – is often measured by a two step procedure that make use of both meteorologic data and plume measurements. The first step is to determine the amount of gas in a cross-section of the plume. This is done by measuring the column density,  $\text{kg/m}^2$  – either using a mobile spectrometer and have it traverse the plume or using a stationary spectrometer and scan the plume. When doing traverses, the telescope is usually pointing in the zenith direction while scanning measurements points in a total of almost  $180^\circ$  (from one horizon to the other). The light source is thus not direct sunlight but rather scattered sunlight. While measuring scattered sunlight is usually not a problem, it should be noted that under certain conditions the light path may be suboptimal. This could typically mean that light entering the telescope have been scattered multiple times within the plume (and thus the absorption is over- estimated), or that the light was scattered between the plume and the telescope (thus showing no absorption signal at all). (Galle *et al.*, 2011)

The column density,  $\sigma$ , can be defined as the mass per unit area and is obtained by integrating the density of the substance,  $\rho$  along a certain path, typically the entire atmosphere:

$$\sigma = \int \rho ds \quad (14)$$

In volcanic monitoring it is often the column density in the plume relative to the normal atmosphere rather than the absolute column density that is measured, as the difference corresponds to gases in the plume. The column density is then integrated across the entire plume to obtain the amount of gas in a cross section,  $\text{kg/m}$ .

The next step is to use this information in combination with the wind speed,  $\text{m/s}$ , in the plume in order to get the flux. By multiplying the amount of gas in a cross section with the wind speed the flux,  $\text{kg/s}$ , is obtained.

### 2.4.1 Making traverses using a mobile spectrometer

Using a mobile spectrometer and traverse the plume is the conceptually easiest method, although it may not always be the most feasible when in field. The basic idea is to measure the column density not only for a single column but rather for an entire cross-section of the plume and integrate along the traverse in order to get the number of molecules in the cross-section,  $\text{kg/m}$ , which is later multiplied by the wind speed to get the flux.

The spectrometer is mounted on a moving platform, typically a car, and alinged to measure the column density of the gas in the zenith direction. As the platform is moving across the plume, spectra are collected and the column density is calculated using these spectra. As a reference, a spectra is collected outside of the plume where the volcanic gas content should be zero.

In the ideal case, the traverse is made along a line perpendicular to the wind direction, and the resulting column density is then integrated over the distance traveled during the acquisition. However, in any real case it may often not be possible to make the traverse along a straight line perpendicular to the wind direction. Instead, the distance traveled has to be projected onto a line

perpendicular to the wind direction. This can be seen in figure 3. The distance is projected since it is the amount of gas in a cross section perpendicular to the wind direction that is multiplied with the wind speed in order to calculate the flux. Worth noting is that the sign should be kept during the projection in case the road used for making the traverse at some point goes backwards through the plume.

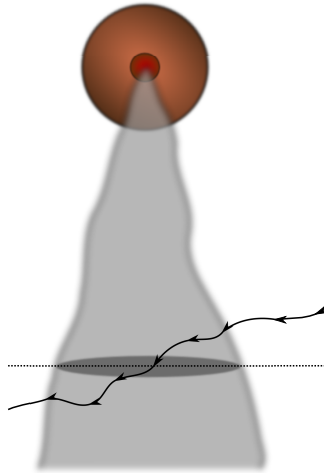


Figure 3: This figure shows an ideal traverse (the dotted line) – where the traverse is going in a straight line perpendicular to the wind direction – as well as a typical traverse (the solid line). In the latter case, the distance has to be projected onto a line perpendicular to the wind direction.

The idea of calculating flux by making traverses is a simple principle, however in practice it may not always be as straight forward as it seems. Some of the advantages and disadvantages of traverses are listed below:

- + Simple geometry allows for simple flux calculation
- + No stationary equipment is needed
- + If there are roads surrounding the volcano, measurements can be done regardless of wind direction
- If there are no roads surrounding the volcano, doing traverses can be hard
- Requires resources in terms of vehicle, gas and personnel
- Winds may change during the traverse, resulting in fluxes being either over- or under-estimated

#### 2.4.2 Scanning the plume using a stationary spectrometer

Sometimes, using a mobile spectrometer to run traverses under the plume is not feasible. This may be due to lack of suitable roads or lack of the time and resources. In those situations installing a stationary spectrometer and instead

scan the plume might be a better choice. Besides, installing a stationary spectrometer is a much better way to ensure continuous measurements as the system can be automated and set to run by itself.

The general idea behind a scanning system is to change the pointing direction of the telescope between each collected spectrum rather than maintaining the same looking angle while altering the position. By doing this, the entire plume can be scanned and measured from a fixed position.

One of the problems that occur when using a stationary spectrometer to scan the plume is that the geometry becomes more complex and requires additional information about the plume. This is because the stationary spectrometers scan with a discrete angular step and therefore the amount of gas between two steps is different, depending on whether the plume is far away from or close to the spectrometer. This can be seen in figure 4. Because of this, the plume height is required in order to calculate the flux with this setup.

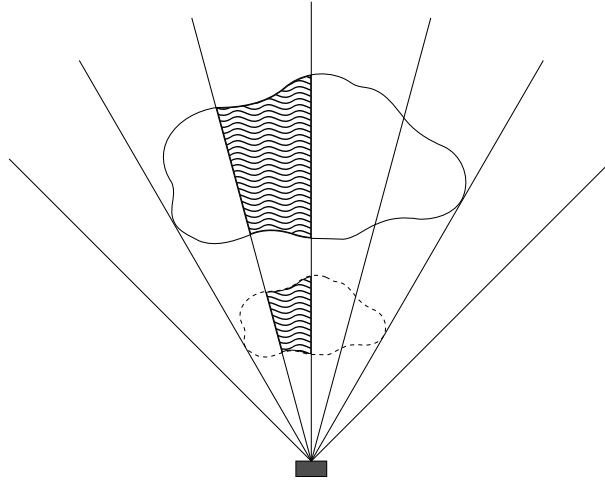


Figure 4: An example to show that the scanning instrument can not distinguish a low and narrow plume from a high and wide plume. If the plume height is not known it is not possible to calculate the total amount of gas in the plume.

The full derivation of the expression for the flux will not be given here, but the general idea is to calculate the average column between two scan angles as well as the corresponding distance between each scan at the height of the plume. The plume gas content is then integrated for each scan angle to obtain the complete plume, which is then multiplied with the wind speed as well as a geometry factor that accounts for wind direction and positioning of the instrument.

In order to obtain the plume height, more than one stationary spectrometer can be used. If several spectrometers see the plume, the plume height is calculated by first determine the center of the plume as seen from each spectrometer. The intersection between the lines from each spectrometer towards their calculated plume center then gives the plume height by triangulation. Some of the advantages and disadvantages of plume scanning are listed below:

- + Once installed properly a stationary spectrometer can run un-attended
- + Automated measurements produces long time series at low additional cost

- + Relatively fast measurements gives good time resolution
- Can only cover a limited span of wind directions unless a large number of spectrometers are installed
- Complex geometry complicates flux calculation
- Requires plume height data which requires that two spectrometers see the plume

One obvious drawback with a stationary spectrometer is that when the wind is blowing in certain directions it is not possible for the spectrometer to see the plume. In order to overcome this problem with a minimum number of additional spectrometers a new scanning technique was developed. Instead of using a scanning angle of  $90^\circ$  and scan a plane, a scanning angle of  $60^\circ$  is used, thus scanning a cone. The benefits of the conical scanning is that it allows for better coverage with the same number of spectrometers, at the cost of a yet more complex geometry.

### 3 Mini-DOAS instruments and software

This chapter describes the implementation of the mobile and scanning DOAS techniques described in chapter 2. The softwares used are briefly explained in section 3.1, followed by a description of the mobile and scanning DOAS systems in sections 3.2 and 3.3. Modifications to the scanning mini-DOAS instrument to make it more suitable for high latitude volcanoes are proposed and discussed section 3.4.

#### 3.1 Software: MobileDOAS and NOVAC Program

As a part of the NOVAC project, two different softwares were developed: MobileDOAS and NOVAC Program. The MobileDOAS software is responsible for both collecting and processing data when doing traverses. The NOVAC Program is on the other hand responsible for automatic downloading and processing of the data from the NOVAC stations, as well as uploading this data to the central server at Chalmers. The NOVAC Program is thus a key ingredient in the global volcanic gas emission monitoring network.

In both softwares the DOAS processing is done in a very similar way and both follow the procedures described in chapter 2. In the configuration, the user has the option to specify reference spectra and their corresponding fit region (i.e. the wavelength to pixel mapping) as well as shift and squeeze parameters. Some other configuration options related to the DOAS evaluation process are also available, such as the choice of sky and dark spectrum.

#### 3.2 Mobile DOAS

The setup used for mobile mini-DOAS measurements consists of:

- Laptop running the MobileDOAS software
- Spectrometer (USB2000, a compact version of the S2000) connected to the laptop
- Telescope connected to the spectrometer using optical fibre
- GPS receiver connected to the laptop via USB

When performing mobile DOAS measurements the MobileDOAS software is first configured by providing reference spectra (typically  $\text{SO}_2$ ,  $\text{O}_3$  and a ring spectra) and their corresponding shift and squeeze. Also, the region in which the reference spectrum should be fitted is specified, given in channel numbers. For this application, wavelengths between 310 nm and 325 nm are used and the corresponding channel numbers are typically obtained once during the calibration process.

The last step in the configuration is to specify exposure time for the measurement, as well as the desired time resolution. The exposure time can be set either manually or automatically. If automatic exposure time calculation is used, the exposure time is obtained by first collecting a spectrum from which a suitable exposure time is calculated. The total number of spectra averaged in each measurement is then given by dividing the time resolution with the exposure time and round down.

If automatic exposure time is used, the telescope first has to be pointed towards the sky to calculate the exposure time to be used. If manual exposure time is used, the first step is skipped. A dark spectrum is then collected by covering the telescope. During the traverse, the GPS receiver logs the position for all collected spectra and the position and spectral data is processed by the MobileDOAS software. With the addition of meteorologic data, the flux can then be calculated as described in section 2.4.1.

### 3.3 Scanning mini-DOAS

The most common version of the scanning mini-DOAS system used in the NOVAC project consists of the following equipment:

- The scanner, with the following parts:
  - Scanner body, typically mounted on top of a pole to improve vision
  - Rotating hood with a quartz window
  - Mirror or prism (either  $90^\circ$  or  $60^\circ$ )
  - Telescope with a field of view of 8 mrad
  - Stepper motor to control scan direction by rotating mirror and hood
- Quartz optical fibre connecting the scanner to the spectrometer
- S2000 spectrometer from Ocean Optics Inc.
- GPS receiver
- Thermometer
- Antennas and radio or satellite links for communication (not always present)
- Embedded PC to control the scanner, collect spectra and handle data communication

In addition to the equipment listed above the system needs some kind of power source. As the NOVAC systems – by design – have a very low energy consumption, connecting a solar panel, a regulator and a battery is usually sufficient in the equatorial regions. Other solutions include wind power and utilizing land lines, if present.

In figure 5, a schematic view of the dual beam scanning mini-DOAS system can be seen. The dual beam scanning mini-DOAS has the ability to measure the wind speed of the plume if the plume is detected right on top of the scanner. This is done by correlating measured column at two different points within the plume (along the wind direction) and calculate the time needed for changes in the column to propagate from the upwind measurement point to the downwind measurement point. If the plume height is known, the distance between the two points can then be calculated. Combined with the time difference in the measured column the wind speed in the plume can then be obtained.

The major difference of a dual beam system compared to a single beam scanning mini-DOAS is that the dual beam scanner requires two spectrometers or, in practice, the double SD2000 spectrometer. The wind speed measurements

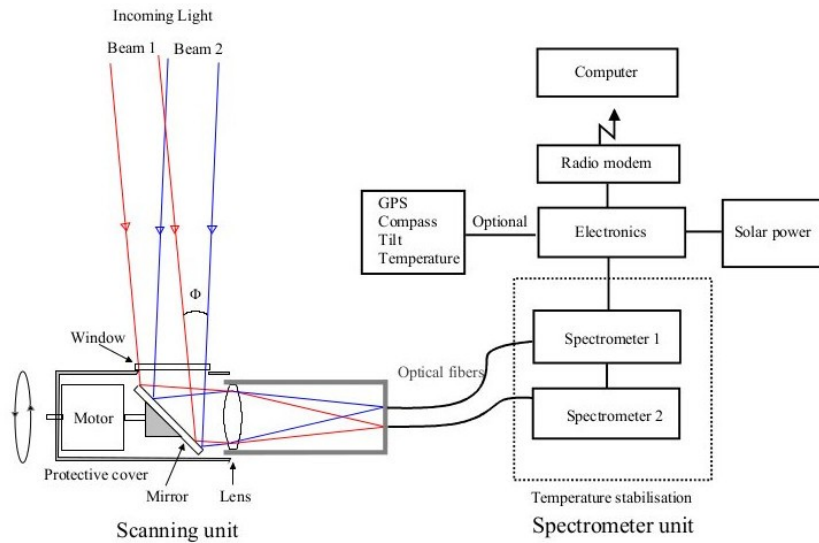


Figure 5: Schematic view of the dual beam scanning mini-DOAS system. The principle behind the single beam system is the same, but it only has one set of fibre and spectrometer.

require that the scanner is looking in the zenith direction so it is not possible to use a conical scanner with the dual beam scanner (Johansson *et al.*, 2009).

Configuration of the system is done for each station via configuration files in the embedded PC. Important settings include the cone angle, the delay between each scan, the compass direction of the scanner, various parameters related to the spectrometer as well as a list specifying which measurements to be done (sky, dark and which scan directions to be used). Under normal circumstances the exposure time is set to automatic and a spectrum is first collected to calculate a suitable exposure time. After this, a sky spectrum (sometimes referred to as the *Fraunhofer reference spectrum*) is collected as well as a dark spectrum. The dark spectrum is collected by simply pointing the mirror downwards, thus blocking the vision of the sky. The next step is to scan the plume, usually by doing a  $180^\circ$  scan in steps of  $3.6^\circ$ . If clear view of the the sky is blocked in certain directions, e.g. by a tree or a mountain, scan directions can simply be excluded in the configuration file.

### 3.4 Modifications of the scanning mini-DOAS instrument to better suit high latitude volcanoes

High latitude volcanoes will be characterized by significantly different conditions compared to volcanoes in the equatorial region. Because of their high latitude, the solar elevation angle may be low even at mid day. As UV light (especially UVB and UVC) is strongly absorbed and scattered by the atmosphere, the longer path caused by the lower solar elevation angle means that less UV light will reach the spectrometer. Instruments installed to monitor volcanoes found in high latitude areas are thus affected by seasonal changes to a higher degree, as

both the seasonal changes in the weather and the changes in light are stronger. The weather might also become a concern with snow and temperatures below freezing. In order to handle the problems that might occur, a few modifications of the current scanner setup have been implemented and, to some extent, tested.

### 3.4.1 Replace rotating hood with a quartz cylinder

In order to protect the telescope, the motor and the mirror in the scanning mini-DOAS instrument, they are covered by a hood with a small quartz window. As the mirror, and thus the looking angle, is rotating during the scan, the hood with the quartz window also needs to rotate and it is therefore attached to the motor. There are a number of both potential and real problems with this setup, namely:

- Since the hood has to rotate the total moment of inertia is higher. As a result, the stepping motor will need a longer time to complete a full step in order to avoid damage and misalignment. This will effectively work as a constrain on how fast a scan can be done, lowering the temporal resolution.
- Moving parts increases the risk of parts getting stuck or events that otherwise result in breakdown. The scanner case needs to have enough margin to be able to rotate in spite of dust, dirt, ice or small misalignments.
- The abovementioned margins doesn't allow for the case to be sealed, which will let acid rain and acidic particles to enter the cavity and corrode both the mirror as well as the lenses in the telescope.

In an attempt to improve the the scanning mini-DOAS and to address the problems mentioned above, a new scanner prototype has been developed. Rather than having a small quartz window, the entire rotating hood is instead replaced by a static quartz cylinder that gives the telescope sky vision without having to rotate. Benefits of using a static quartz cylinder includes lower moment of inertia, better sealing properties and a lower number of moving parts. The new scanner prototype can be seen alongside the old (conical) scanner in figure 6.



Figure 6: The old conical scanner with a rotating hood and a small quartz window can be seen to the left and the prototype scanner with a non-rotating quartz window can be seen to the right.

In the configuration files for the scanner, the parameter `MOTORDELAY` sets the number of milliseconds to wait between each pulse sent to the stepper-motor. The default (or rather: recommended value) is 200 ms for the flat scanner and 500 ms for the conical scanner. Experience has shown that the use of a shorter delay may cause damage to the equipment in the long term as the stress on the motor will be high. In addition, the fast rotation may cause the hood to start slipping and become misaligned. By replacing the rotating hood with a stationary quartz window, it should be possible to shorten the delay between each step significantly.

The motor used has an angular step size of  $1.8^\circ$ , which gives a total of 200 steps per full rotation. In a typical scan, the motor has to make a total of two rotations, or 400 steps, as it first will collect sky and dark spectra and then do a full  $180^\circ$  scan. For the flat scanner, this results in a total delay of 80 s while the conical scanner gets a total delay of 200 s. Typically under normal conditions the spectrometer uses an integration time of 300 ms and averages 15 spectra in 52 different directions (sky, dark and a step size of  $3.6^\circ$  for a  $180^\circ$  scan) which means that the theoretical minimum time required for a full scan will be 314 s for the flat scanner and 434 s for the conical scanner.

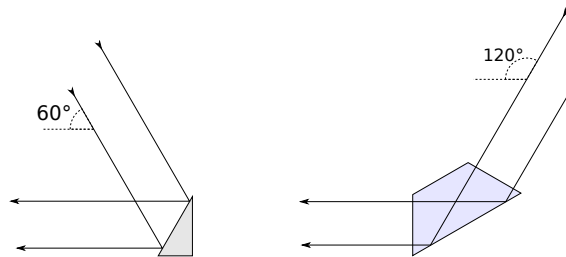


Figure 7: If the mirror of the conical scanner would be replaced by a prism, it would reflect light from an angle of  $120^\circ$  rather than  $60^\circ$ . The bulkiness of the prism is also apparent in this figure.

In the case of a flat scanner, problems with corroded mirrors can easily be solved by replacing the mirror with a quartz prism, as it is more resilient towards the corrosive effects. At the current stage, this is not feasible with the conical scanners. The first problem that occurs when trying to replace the conical mirror with a prism is that a prism will reflect light from a  $120^\circ$  angle rather than a  $60^\circ$  angle.

In theory, this can be solved by simply rotating the scanner  $180^\circ$  in the horizontal plane. In practice, this solution is not preferred since the data would have to be treated differently compared to the other NOVAC stations. As one of the ideas within the NOVAC project is to focus on simplicity, an additional layer of complexity and potential confusion is not desired and at present. Replacing corroded mirrors should instead be considered a part of regular maintenance work on conical scanners. Additionally, a  $120^\circ$  prism will be more bulky and may not fit the current scanner housing, something that partly can be reduced by not using a full triangular shape but only an isosceles trapezium. A comparison of the light path between the currently implemented mirror and a prism can be seen in figure 7. From this figure it is also apparent that a prism will be more bulky than a mirror. In practice, the main reason that this solution has not yet

been implemented is that a re-design of the instrument is needed and that such a prism is not an easily obtained item as it is not a standard product.

### 3.4.2 Replacing the S2000 with the Maya2000 Pro spectrometer

Today, the spectrometer used in the NOVAC stations is the S2000 from Ocean Optics. In order to better handle the situation with lower light, a new spectrometer with higher sensitivity to UV light has been tested. The new spectrometer is the Ocean Optics Maya2000 Pro, which is supposed to have better sensitivity to UV light.

**Exposure time and column error** In order to compare the Maya2000 Pro spectrometer to the S2000 spectrometer two conical scanner systems were set up in parallel, one with the S2000 and one with the Maya. To get a clear reference of SO<sub>2</sub> in order to simulate a flux and validate the detection limit, a cell containing approximately 100 ppmm of SO<sub>2</sub> were placed on top of the scanner. The data was then processed according to the normal NOVAC Program evaluation procedure. The evaluated flux may not be of great interest, but the error of the column calculation definitely is, as it gives an indication of the quality of the measurement.

SO<sub>2</sub> is evaluated between 310 nm and 325 nm, which is in the tail end of the sky spectrum before basically all light goes extinct somewhere around 290 nm. Because of this, the intensity in the fit region drops very fast as the sun nears the horizon. This is expected to be seen in measurements, as the decreased intensity in the fit region will lower the signal-to-noise ratio and increase the errors.

While the Maya2000 Pro spectrometer has a higher sensitivity to UV light, the exposure time used in measurements is still calculated for the peak of the collected spectrum rather than the level of saturation in the UV region. Thus, the calculated exposure time may not necessarily reflect this improved sensitivity. However, it is still interesting to compare the calculated exposure times for the Maya and the S2000 spectrometers as the exposure time is one of the major limitations to faster measurements and higher temporal resolution. It is also interesting to see at which time of the day an exposure time of 1000 ms is reached, as it is used as the maximum exposure time at most NOVAC stations.

**Wavelength misalignment** As discussed in section 2.2.1, one thing that often needs to be considered, and corrected for, when working with spectrometers in DOAS applications is that the wavelength alignment changes over time. This is typically represented by either a shift or a squeeze or stretch in the wavelength-to-pixel mapping, or both. While testing the Ocean Optics Maya2000 Pro spectrometer to evaluate its potential as a replacement for the S2000 spectrometer, it turned out that the Maya spectrometer seems to be more sensitive to temperature changes when it comes to wavelength misalignment. This behaviour was discovered while doing detection limit tests, where the spectrometer (unintentionally) was exposed to cold air. While evaluating the test data, a strong offset was observed in the measured SO<sub>2</sub>-column before and after the spectrometer got exposed to the cold air.

To test the high sensitivity to temperature changes in the wavelength alignment, a telescope was set to point towards the sky measuring only the column

in a gas cell. The cell contained 100 ppmm of  $\text{SO}_2$  and the measurements were done during approximately two hours, using an exposure time of 1000 ms collecting a spectrum every 5 s. The spectrometer was placed in room temperature (estimated  $21^\circ\text{C}$ ) with a fibre to the telescope on the outside (estimated  $-5^\circ\text{C}$ ) with the window left ajar. After approximately 600 collected spectra, the window was opened wide and the spectrometer got exposed to cold air for about five minutes after which the window was closed again. The same thing was repeated after approximately 1700 measurements. The  $\text{SO}_2$ -column was then calculated both with a fixed shift for all spectra and with individual shifting of each spectrum against the aquired sky spectrum.

## 4 Test results for the Maya2000 Pro

### 4.1 Results: exposure time and column error

As discussed in section 3.4.2, a noticeable increase in the signal-to-noise ratio should be expected as the solar elevation angle gets lower. This behaviour can easily be seen in figure 8, where the error in the calculated  $\text{SO}_2$  column is at a minimum at noon and increases the closer to dusk or dawn you get. The data included in the figure is data that is considered a good point by the NOVAC Program and that has a fit saturation of at least 9%.

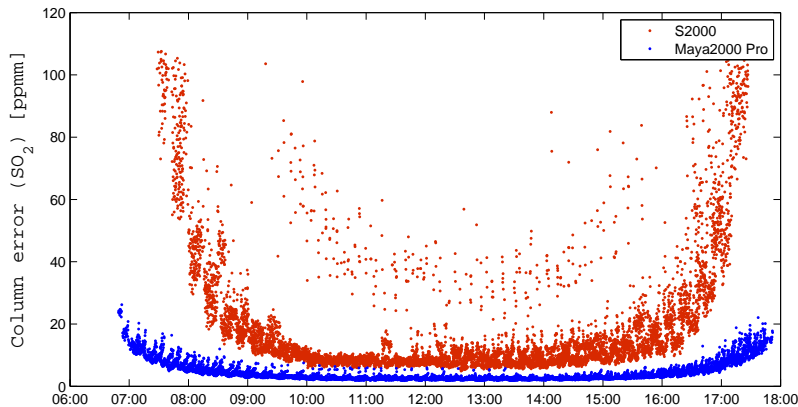


Figure 8: Diurnal variation of column error in the estimation of  $\text{SO}_2$  for the S2000 and the Maya between March 7 and 11.

Data was collected between March 7 and March 11 as described in section 3.4.2. The weather during these days was relatively good with mostly clear sky. The sunrise and sunset in Gothenburg at March 9 was 06:45 and 18:00, respectively. During those conditions we see that the Maya was able to produce measurements with a column error below 20 ppmm within 20 minutes after sunrise and until 20 minutes before sunset, while the same figures for the S2000 is above two hours at each end. Also noticeable is the considerably lower error of the Maya during mid-day.

As seen in figure 9, the calculated exposure time from the same dataset is lower for the Maya compared to the calculated exposure time for the S2000 at basically all times during the day. For measurements where both exposure times drop below 1000 ms, the calculated exposure time of the Maya spectrometer is typically 200-300 ms lower compared to the S2000. Worth noting is that the calculated exposure time of the Maya spectrometer goes below 1000 ms approximately 45 minutes earlier in the morning and reaches 1000 ms approximately 45 minutes later than the S2000 spectrometer.

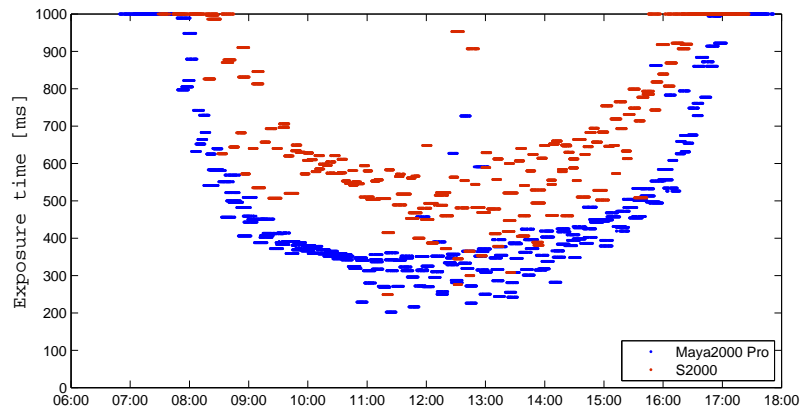


Figure 9: Diurnal variation of calculated exposure time for the S2000 and the Maya between March 7 and 11.

## 4.2 Results: wavelength misalignment

The results in figure 10 show that there is a strong correlation between a shift in the wavelength-to-pixel mapping and a systematic error in the evaluated  $\text{SO}_2$  column (the red dots). After correcting for this shift, the re-evaluated  $\text{SO}_2$  column (the blue dots) much better reflects the 100 ppmm  $\text{SO}_2$  in the gas cell that was used as a reference. The strong changes in the shift (the black line) seen in figure 10 can be explained by semi-controlled changes in the conditions in the lab. The sudden drop seen around 600 measurements happened as the window next to the spectrometer was opened wide for approximately five minutes, exposing the spectrometer to the cold air (approximately  $-5^\circ\text{C}$ ), forcing the spectrometer to cool. The same thing was repeated towards the end, around measurement 1700, but at this time the intensity had dropped so low that the noise level made it harder to directly see a correlation between wavelength misalignment and an error in the measured column.

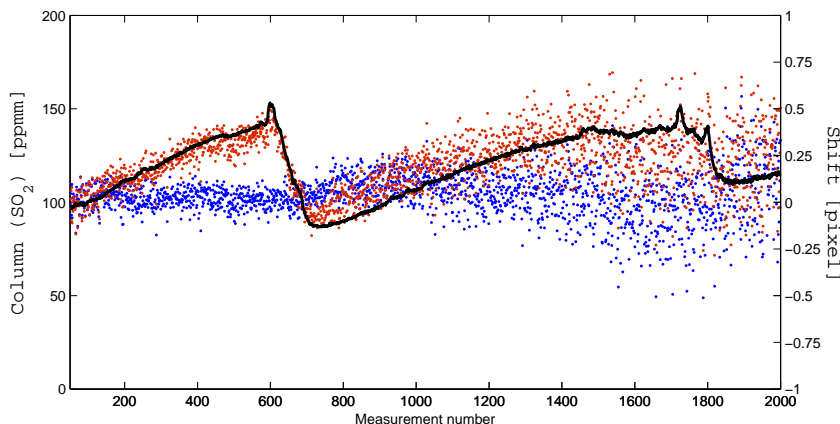


Figure 10: Evaluated column from measurements on a gas cell with 100 ppmm  $\text{SO}_2$ . The blue dots corresponds to data where corrections of shift for individual measurements were performed during the processing and the red dots corresponds to data without such corrections. The black line corresponds to the calculated shift. At measurement numbers close to 600 and 1700 the window was opened to force cooling of the spectrometer.

Data on the actual temperature of the spectrometer is not available, but a good way to display the relationship between a shift in the wavelength-to-pixel mapping and the error in the  $\text{SO}_2$  column estimation if this shift is not adjusted for can be seen in figure 11. The  $\text{SO}_2$  column should be measured to 100 ppmm but as the shift gets larger the calculated value starts to deviate with up to 40 ppmm at a shift of 0.5 pixels.

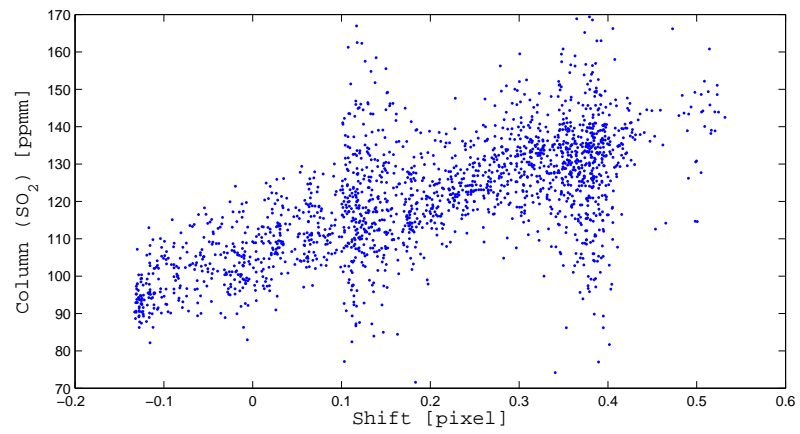


Figure 11: Evaluated column of SO<sub>2</sub> without correcting for shift as a function of the calculated shift for each measurement.

## 5 Field campaign at Telica, Nicaragua

In the May 2011 campaign both stationary mini-DOAS flux measurements and MobileDOAS flux measurements were conducted. On May 23 the two stationary rapid deployment system instruments were installed and were kept running until June 17 and June 24, respectively. It should be noted that one of the spectrometers was knocked over by livestock and remained misaligned for a few days somewhere between June 13 and June 17.

The second stage of the 2011 field campaign at Telica consisted of making additional measurements by doing traverses using a mobile spectrometer. Those measurements were to serve as a complement to the measurements from the scanning spectrometers. During a total of nine days between May 24 and June 17 traverses were done.

### 5.1 Scanning mini-DOAS measurements

During the May 2011 campaign only two sets of single beam scanning mini-DOAS were installed – one conical and one flat scanner – as compared to the three sets installed during the late 2009 to early 2010 field campaign. The reasons behind this decision were mainly of practical nature. Also, using statistics for the wind distribution obtained during the last field campaign, two spectrometers were deemed sufficient.



Figure 12: The two sites where the rapid deployment systems were installed. To the left is the conical scanner at Mendoza and to the right is the flat scanner at Los Angeles. A map showing their locations can be seen in figure 13.

The two sites used in this campaign were Mendoza and Los Angeles, both used in the previous campaign. Photographs showing the installations can be seen in figure 12 and the location of the two sites can be shown in figure 13. Worth noting is that the spectrometers does not need to have direct vision of

Table 1: Scanner type, setup and location of the two stationary spectrometers used to monitor Telica.

	Mendoza	Los Angeles
<b>Scanner type</b>	Conical, 60°	Flat, 90°
<b>Compass direction</b>	86°	68°
<b>Latitude</b>	12.5981	12.5781
<b>Longitude</b>	-86.9021	-86.8986
<b>Altitude</b>	230 m	217 m
<b>Serial number</b>	D2J2205	I2J7212

the volcano itself, since it is only the plume above the spectrometer that is measured. However, it still has to be properly aligned to scan perpendicular to the direction of the volcano. For more information on the two sites, please see table 1. In table 1 the altitude is expressed in meters above sea level and the compass direction is the direction from the station towards the volcano, expressed in positive degrees clock-wise from north.

Even though the rapid deployment system allows for data transfer both over satellite link and by the use of radio modems, those features were not utilized. Instead data was collected from the stations manually using FTP over ethernet. The satellite link was excluded due to high cost and the radio modems were excluded because the extra work needed to set up and install antennas was not worth it since the stations easily could be visited when doing traverses.

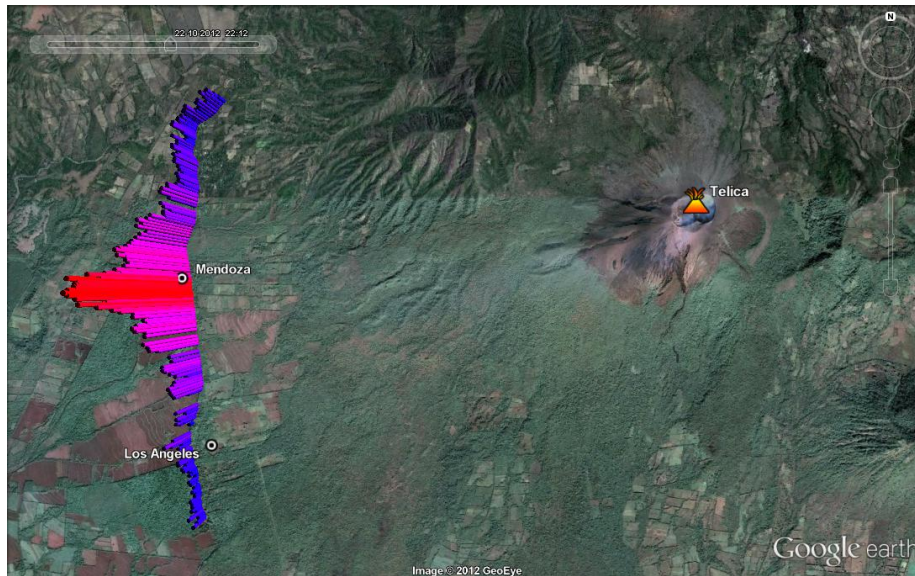


Figure 13: Map showing the volcano Telica as well as the two sites where spectrometers were installed: Mendoza and Los Angeles. Measurement results from one of the many traverses are also shown. Image from Google Earth.

## 5.2 Mobile mini-DOAS measurements

As a complementary stage to the May 2011 measurement campaign at Telica, it was decided to do traverses using a mobile spectrometer and the MobileDOAS software.

As the winds were mostly easterly, a majority of the traverses were done on the western side of the volcano. The road on the western side is a dirt road connecting the small villages and farms and it is also partly covered by foliage. As a result it could be hard at times to get proper exposure of the spectrometer, as the sky would be obscured by the foliage. To the left in figure 14 the effects on spectrometer saturation are distinct, as the spectrometer is near saturation when the telescope has clear vision of the sky, whereas heavy influence of foliage lowers the saturation significantly as well as introducing noise. This can be accounted for by simply removing low intensity points manually. However, this is also effectively lowering the spatial resolution, as seen to the right in figure 14.

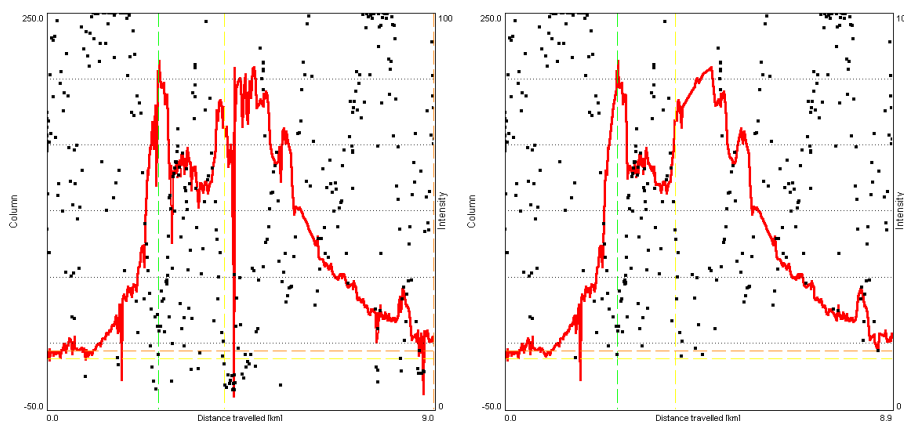


Figure 14: An example showing how the saturation of the spectrometer (black squares) is greatly affected by foliage along the road on the west side of Telica. To the right these low intensity points have been removed, at the cost of a lower spatial resolution. The red line shows the measured  $\text{SO}_2$  column.

The total time needed to perform a full traverse under the circumstances at Telica was usually between 20 and 30 minutes, depending on wind direction and road condition. During this time the wind direction could change up to  $10^\circ$ , as seen in figure 15 which is picturing the measured wind direction for June 1. As briefly discussed in section 2.4.1 these changes in wind direction during traverses might cause over- or under-estimation of the actual plume size which will result in errors in the flux calculation. Because of this, several traverses were often done in rapid succession in order to get an average to minimize these effects.

## 5.3 Wind speed data

The wind speed data used in the flux calculations for both mobile and scanning DOAS measurements came from two different sources: measured wind speed directly by INETER at Telica as well as archived wind speed data from the GDAS1 (Global Data Assimilation System) model from NOAA (National

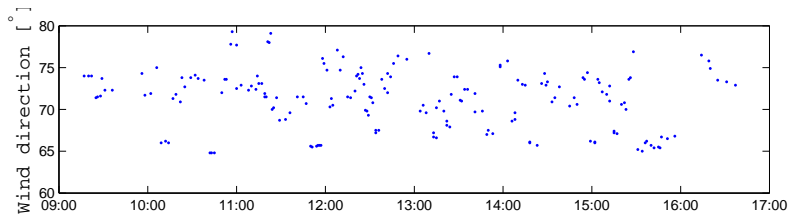


Figure 15: Measured wind direction for June 1 showing the variations in measured wind directions over the day. Quick variations in wind directions, as seen here, may cause problems when doing traverses.

Oceanic and Atmospheric Administration). While the data obtained from INTER has a 5 minute temporal resolution, there are still occurrences where no data is available. In those occasions wind speed data from NOAA had to be used. The GDAS1 data has a much lower temporal resolution of 3 hours.

When working with the GDAS1 model, the location at which the wind speed should be retrieved needs to be supplied. From the NOAA website, the wind speed at a given number of altitudes at a certain longitude and latitude can be obtained. This data then needs to be interpolated in order to get the wind speed at the height of the plume.

## 6 Results from the field campaign at Telica

Results from both scanning mini-DOAS measurements and mobile DOAS measurements acquired during the field campaign at Telica will be presented in this chapter. As discussed in section 2.4.2, the flux can only be properly calculated if the plume height, wind speed and wind direction is known. Before the wind speed can be extracted the plume height has to be known (see section 5.3). The plume height was obtained by geometric calculations that required both scanning DOAS stations to see the plume (Johansson, 2009). Using the calculated plume height, the wind direction was then obtained. The plume height and wind direction measured in the May 2011 field campaign can be seen in figure 16 and 17.

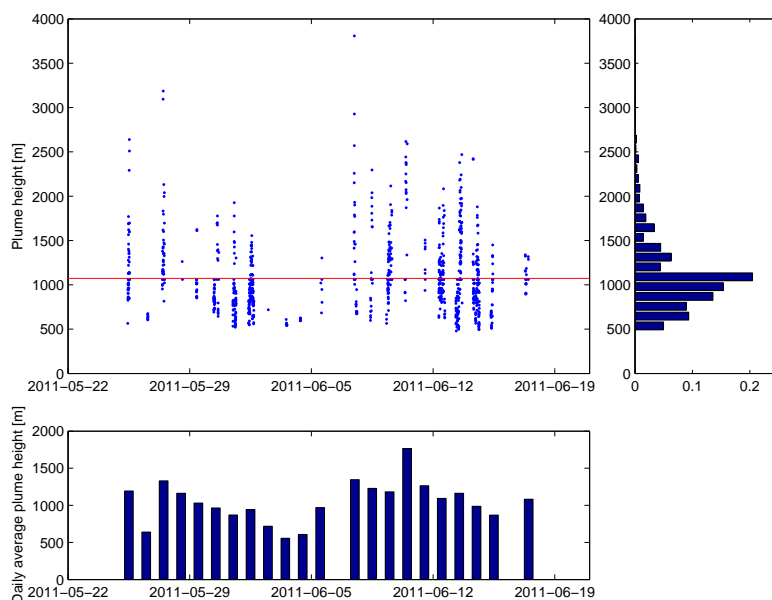


Figure 16: Measured plume height (above sea level) at Telica between May 25 and June 24. The red line is the average plume height of 1073 m. The histogram to the right shows the plume height distribution. Below is the daily averages.

The average measured plume height during the campaign was  $1073(\pm 393)$  m (above sea level), although peak plume heights above 3000 m were recorded. As a reference, the crater is positioned at an altitude of 1061 m. As we can see in the histogram in the right side of figure 16, the measured plume heights are mainly distributed between 600 m and 1100 m while plume heights above 1100 m seems less common and wider spread. The daily plume height averages in the lower part of figure 16 shows that even if individual peak plume heights can be a lot higher, the average still mostly resides between 500 m and 1500 m.

Wind directions measured during this campaign can be seen in figure 17. These measurements shows that the wind direction fluctuates between  $60^\circ$  and

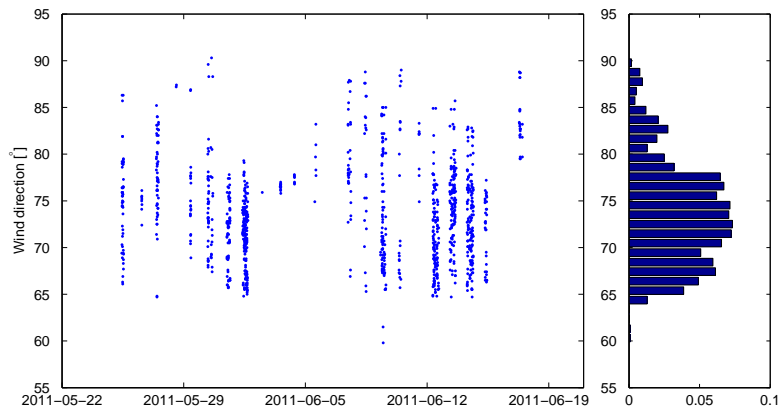


Figure 17: Measured wind direction at Telica between May 25 and June 24. Note that the figure only displays angles between  $55^\circ$  and  $95^\circ$ . The distribution of measured wind directions can be seen to the right.

$90^\circ$  with an emphasis between  $65^\circ$  and  $80^\circ$ . It should not be forgotten that only wind directions that allows both stations to see the plume can be measured.

Using the wind data obtained, the flux can be calculated. Daily averages of the flux measurements from the two stationary spectrometers can be seen in figure 18. The average measured flux over the entire campaign is  $143(\pm 109)$  t/d, while the daily averages ranges from 17 t/d to 260 t/d.

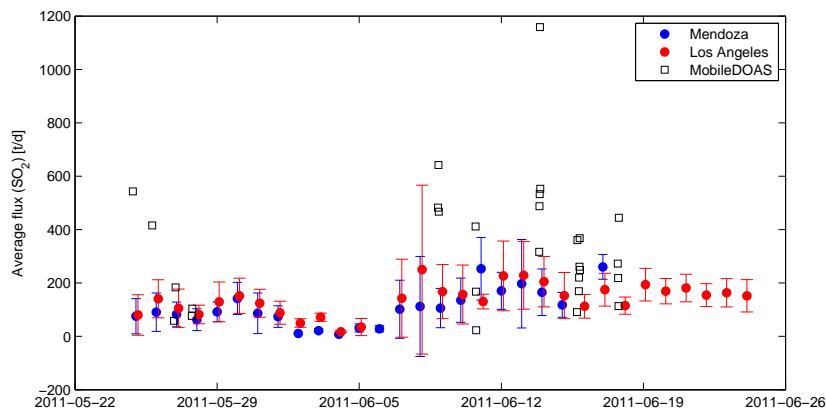


Figure 18: Daily averages of flux measured at Telica using scanning mini-DOAS instruments seen in red and blue. The black squares corresponds to the Mobile-DOAS measurements.

As daily averages does not capture certain features, such as eruptive or heavy degassing events, it is also interesting to look at the daily variations. In figure 19, all unique flux measurements can be seen. From this figure it

is apparent that even if the average daily flux is below 200 t/d, peaks in the measured flux can reach well above 1000 t/d and that there is an increased level of degassing between June 7 and June 14.

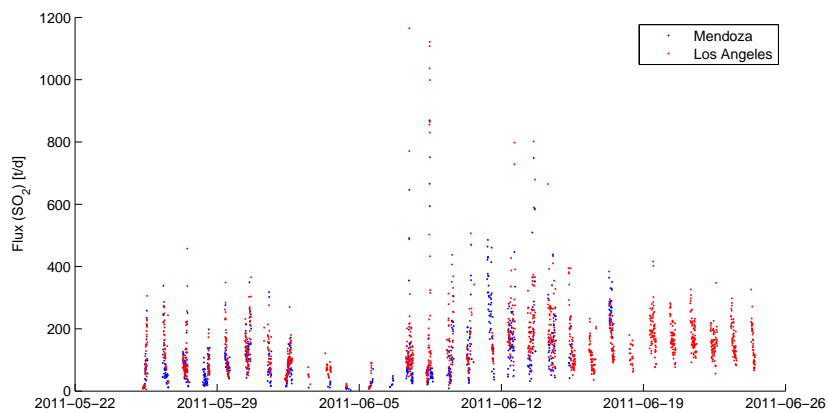


Figure 19: Flux measurements at Telica between May 25 and June 24. From this data, a couple of heavy degassing events between June 7 and June 14 could easily be detected.

The results from the mobile DOAS measurements can be seen in figure 18. The general trend in the results from the traverses is that they seem to show higher flux compared to the scanning DOAS measurements. The average measured flux for the traverses done between May 24 and June 17 is  $335(\pm 237)$  t/d.

## 7 Conclusions and discussion

### 7.1 Instrument modifications

The main goal of this thesis was to modify the current scanning mini-DOAS instrument to become better suited for use at high latitude volcanoes. As a part of this work the new Maya2000 Pro spectrometer was tested in order to see if it provided an improvement over the S2000 spectrometer in conditions where the intensity of scattered UV light is low.

When it comes to the suitability of the Maya spectrometer for use at high latitude volcanoes, it showed very promising results. Where the S2000 only presented column errors below 20 ppmm between 09:00 and 16:00 during the testing period in March, the same figures for the Maya was right after 07:00 almost up until 18:00. This gives a total extra time of almost four hours each day where good measurements can be made. In addition the Maya produced measurements with much better error levels during mid-day. It should also be noted that the chosen value for the column errors of 20 ppmm was in fact just the highest measured error for the Maya in the testing period.

Another way to demonstrate the improved performance when using the Maya is to look at the exposure time needed for the Maya, as compared to the S2000. The Maya not only systematically required a shorter exposure time, allowing it to have reasonable exposure time for a longer period each day. It also has a higher sensitivity to UV light, meaning the saturation level in the fit region will be higher for the same exposure time.

During testing of the Maya spectrometer, it turned out that it was more sensitive to temperature changes compared to the S2000 spectrometer. This sensitivity was manifested as a misalignment in the wavelength-to-pixel mapping, or more specifically a shift, which caused an error in the evaluated column. While these variations in the wavelength misalignment may seem to cause significant errors at first glance, it should not be forgotten that the testing setup exposed the spectrometer to a considerable change in the surrounding temperature in a very short time period.

In practice, the temperature changes of the spectrometer within the time window of a scan for scanning DOAS applications is extremely low in comparison and this increased sensitivity should not cause problems for this application. However, it may still cause problems when doing traverses with a mobile DOAS system. The reason for this is partly because of the (usually) longer time it takes to complete a traverse, but also because traverses may be done from within a vehicle with air conditioning. The outside temperature may vary from below freezing at high latitude or high altitude volcanoes to well above 40°C at equatorial region volcanoes. Thus, the sensitivity to this temperature depending shift in the Maya spectrometer must most likely be adjusted for if it is to be used for mobile DOAS traverses with good results.

As of today, the MobileDOAS software is not capable of doing calculation of and correction for shift for each individual spectrum during the evaluation process. As seen from this initial testing of the Maya spectrometer, it definitely should be considered for implementation in future versions of the MobileDOAS software if the Maya spectrometer is to be used for traverses.

Since the Maya spectrometer showed such promising results, two instruments at Hekla, Iceland, has now been equipped with Maya spectrometers instead of

S2000 spectrometers. Results from these stations are pending. In addition, they are also awaiting a replacement of the rotating hood with quartz cylinders.

## 7.2 Field campaign at Telica

The results from the scanning mini-DOAS instruments from the field campaign at Telica did not show any significant changes in SO<sub>2</sub> flux, as compared to the previous field campaign. Although it does show a short period of increased degassing between June 7 and June 13, where a number of possible eruptions can be detected from isolated peaks in the calculated plume height as well as increased gas emissions.

The gas data from this campaign has been subject to further analysis related to the volcanic activity at Telica. Flux data has been analysed in combination with other geophysical parameters in order to describe and understand the state of activity of the volcano. These results can be found in a paper submitted to the Journal of Volcanology and Geothermal Research in March 2013. (Geirsson *et al.*, 2013)

The results from the mobile mini-DOAS measurements does in general present higher values of the measured flux compared to the scanning mini-DOAS. Possible reasons for this include measurements along the meandering of the plume, errors in wind speed data, coinciding traverses and degassing events and manual bias in the selection and detection of plumes and traverses to be evaluated.

As for the meandering of the plume, it could explain some of the higher peaks but it should not show systematic results in the relatively large number of traverses done. However, if meandering is a reason, consecutive traverses could in fact be affected in the same way as it is not unlikely that the meandering period coincides with the time it takes to do a traverse (see figure 15).

## References

- Conde, Vladimir. 2013 (March). *Application of DOAS for studies of evolving volcanic activity in Central America*. Licentiate Thesis, Chalmers.
- Edner, H. et al. 1994. Total fluxes of sulfur-dioxide from the Italian volcanos Etna, Stromboli and Vulcano measured by differential absorption LIDAR and passive differential optical-absorption spectroscopy. *Journal of Geophysical Research-Atmospheres*, **99(D9)**, 18827–18838.
- Finlayson-Pitts, B. J., & Pitts, J.N. J. 2000. *Chemistry of the upper and lower atmosphere*. Academic Press.
- Futurevolc. 2013 (May). *About the project*. <http://futurevolc.hi.is/>.
- Galle, B., Platt, U., Oppenheimer, C., Millán, M., Alonso, L., & Chen, D. 2006 (March). *Development of Optical Remote Sensing Instruments for Volcanological Applications*. Final Scientific Report on EU-project DORSIVA. Chalmers.
- Galle, B., Delgado, H., Garzon, G., Vogel, L., & Platt, U. 2011 (July). *NOVAC, Network for Observation of Volcanic and Atmospheric Change*. Final Scientific Report on EU-project NOVAC. Chalmers.
- Galle, B. et al. 2003. A miniaturised ultraviolet spectrometer for remote sensing of SO<sub>2</sub> fluxes: a new tool for volcano surveillance. *Journal of Volcanology and Geothermal Research*, **119(1-4)**, 241–254.
- Galle, B. et al. 2010. Network for Observation of Volcanic and Atmospheric Change (NOVAC): A global network for volcanic gas monitoring - network layout and instrument description. *Journal of Geophysical Research*, **115(D5)**.
- Geirsson, H., Rodgers, M., LaFemina, P., Witter, M., Roman, D., Muñoz, A., Tenorio, V., Alvarez, J., Conde Jacobo, V., Nilsson, D., Galle, B., Feineman, M. D., Furman, T., & Morales, A. 2013 (March). *Multidisciplinary observations of the 2011 explosive eruption of Telica volcano, Nicaragua: implications for the dynamics of low-explosivity ash eruptions*. Submitted to Journal of Volcanology and Geothermal Research.
- Grainger, J. F., & Ring, J. 1962. Anomalous Fraunhofer line profiles. *Nature*, **193**, 762.
- Hoff, R. M., & Millán, M. M. 1981. Remote SO<sub>2</sub> mass flux measurements using COSPEC. *JACPA*, **31**, 381–384.
- Johansson, M., Galle, B., Yu, T., Tang, L., Chen, D., Li, H., Jin, X. Li, & Zhang, Y. 2008. Quantification of total emission of air pollutants from Beijing using ground based optical remote sensing. *Atmospheric Environment*, **42**, 6926–6933.
- Johansson, M., Galle, B., Zhang, Y., Rivera, C., Chen, D., & Wyser, K. 2009. The dual-beam mini-DOAS technique – measurements of volcanic gas emission, plume height and plume speed with a single instrument. *Bulletin of Volcanology*, **71**, 747–751.

- Johansson, Mattias. 2009 (March). *Application of Passive DOAS for Studies of Megacity Air Pollution and Volcanic Gas Emissions*. PhD thesis, Chalmers.
- Platt, U., & Stutz, J. 2008. *Differential Optical Absorption Spectroscopy: Principles and Applications*. Springer.
- Rivera, Claudia. 2009 (October). *Application of scattered sunlight spectroscopy for quantification of gas emissions from anthropogenic and volcanic sources*. PhD thesis, Chalmers.
- Stoiber, R. E., Williams, S. N., & Huebert, B. 1987. Annual contribution of sulfur dioxide to the atmosphere by volcanoes. *Journal of Volcanology and Geothermal Research*, **33(1-4)**, 1-8.